

## Experimental study on the in-plane thermal conductivity of Au nanofilms \*

CAO Bingyang<sup>1\*\*</sup>, ZHANG Qingguang<sup>1</sup>, ZHANG Xing<sup>1</sup>, TAKAHASHI Koji<sup>2</sup>,  
IKUTA Tatsuya<sup>2</sup>, QIAO Wenming<sup>3</sup> and FUJII Motoo<sup>3</sup>

(1. Key Laboratory for Thermal Science and Power Engineering of Ministry of Education, Department of Engineering Mechanics, Tsinghua University, Beijing 100084, China; 2. Graduate School of Engineering, Kyushu University, Fukuoka 812-8581, Japan; 3. Institute for Materials Chemistry and Engineering, Kyushu University, Kasuga 816-8580, Japan)

Accepted on July 10, 2006

**Abstract** The in-plane thermal conductivity of Au nanofilms with thickness of 23 nm, which are fabricated by the electron beam-physical vapor deposition method and a suspension technology, is experimentally measured at 80—300 K by a one-dimensional steady-state electrical heating method. Strong size effects are found on the measured nanofilm thermal conductivity. The Au nanofilm in-plane thermal conductivity is much less than that of the bulk material. With the increasing temperature, the nanofilm thermal conductivity increases. This is opposite to the temperature dependence of the bulk property. The Lorenz number of the Au nanofilms is about three times larger than the bulk value and decreases with the increasing temperature, which indicates the invalidity of the Wiedemann-Franz law for metallic nanofilms.

**Keywords:** nanofilm, in-plane thermal conductivity, size effect, Wiedemann-Franz law.

Solid thin films with microscale to nanoscale thickness have widely been applied in micro/nano-devices, such as micro-electronics, optoelectronics, and micro/nano-electro-mechanical systems (MEMS/NEMS), due to the rapid advances in nano-science and technology. In most of the micro/nano-devices, the thermal conduction property of the solid thin films is very important to their performance and reliability.<sup>[1,2]</sup> In recent years, metallic nanofilms have been applied to temperature nanosensors, nanoscale heat flow meters<sup>[3,4]</sup>, and high performance thermo-electrical function materials<sup>[5,6]</sup>. Therefore, it is urgently required to investigate the thermal conductivity of metallic nanofilms.

Although the method of molecular dynamics (MD) simulation has been used to study the thermal conductivity of dielectric thin films<sup>[7,8]</sup>, it is very difficult to use the MD method to predict the metallic nanofilm thermal conductivity<sup>[9]</sup>. The reason is that free electrons are the heat carriers in the metallic nanofilms and the MD method can only take into account the transport of phonons rather than electrons. Zhang et al. recently showed that the Wiedemann-Franz law is inapplicable to the Pt nanofilms<sup>[10,11]</sup>, which presents great challenges to the analogy method of indirectly predicting the thermal conduc-

tivity according to the electrical conductivity calculated by solving electron transport equations<sup>[12]</sup>. The difficulty for experimental measurements is how to remove the effects of film contact resistance and heat loss from the nanofilm to its substrate. Zhang et al. put forward a novel method called one-dimensional steady-state electrical heating (1DSSEH) based on a suspension technology and overcame the above bottlenecks. The electrical and thermal conductivities of Pt nanofilms with thickness of 15—40 nm have been reported<sup>[10,11,13]</sup>. In this paper, the in-plane thermal conductivity of Au nanofilms with thickness of 23 nm is investigated by the 1DSSEH method.

### 1 Experiment and measurement details

#### 1.1 Experimental system

The suspended Au nanofilms, shown in Fig. 1, were fabricated by the electron beam-physical vapor deposition (EBPVD) method. The fabrication processes include: (1) A Si (100) wafer with a SiO<sub>2</sub> layer of 180 nm in thickness was used as the starting material. An electron beam resist layer was spin coated to be 320 nm in thickness. By using an electron beam lithography system, the patterns of the nanofilm and the leads were directly drawn on the re-

\* Supported by National Natural Science Foundation of China (Grant No. 50606018)

\*\* To whom correspondence should be addressed. E-mail: caoby@tsinghua.edu.cn

sist. (2) A Cr film of 5 nm and an Au film of 23 nm were deposited subsequently by the EBPVD method. The Cr film was only for adhesion. (3) A liftoff technique was applied, in which the chip was immersed in a liquid resist remover to leave only the Au/Cr pattern on the SiO<sub>2</sub> layer. (4) Isotropic etching using buffered hydrofluoric acid was applied to remove the SiO<sub>2</sub> layer around the nano Au film. The Cr film under the Au film was also etched away in this process. (5) The Si was anisotropically etched out using KOH solution in order to detach the nanofilm from the substrate. It is important to point out that the leads still conglutinate the substrate through the Cr film. Fig. 1 (a) illustrates the fabricated sample structure. Fig. 1 (b) is the image of an Au nanofilm measured by a scanning electronic microscope (SEM). Thus, we can obtain the lengths of the two Au nanofilms of  $l_a = 5.4 \mu\text{m}$  and  $l_b = 5.6 \mu\text{m}$  and the widths of  $w_a = 451 \text{ nm}$  and  $w_b = 455 \text{ nm}$ . The nanofilm thicknesses measured by an atomic force microscope (AFM) are  $d_a = d_b = 23 \text{ nm}$ .

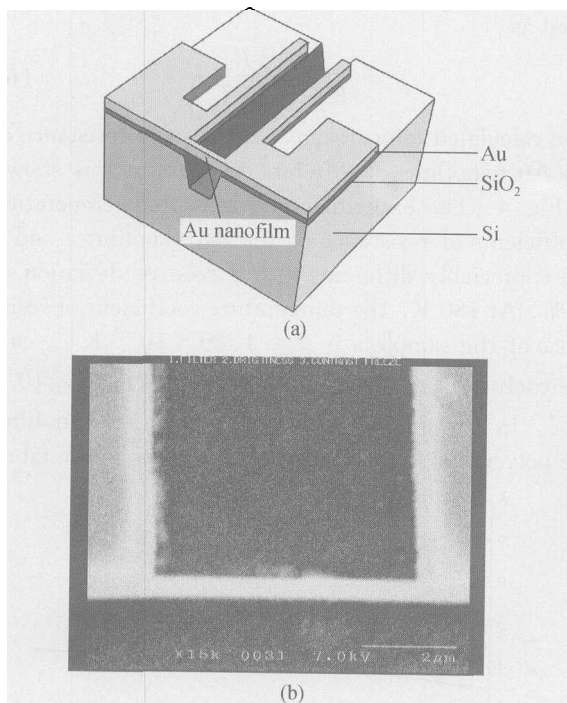


Fig. 1. (a) Schematic diagram of the Au nanofilm sample; (b) scanning electronic microscope image of an Au nanofilm.

The experimental setup measuring the nanofilm thermal conductivity is shown in Fig. 2. The Au nanofilms are fixed on a constant temperature shelf in the liquid nitrogen cryostat. The shelf temperature is controlled by the balance between an electrical heating

and a liquid nitrogen flux being 77—500 K with sensitivity of 0.1 K. The air pressure in the liquid nitrogen cryostat is not more than  $10^{-4} \text{ Pa}$  under control of a series-wound combination of a vacuum pump and a molecular pump. Thus, there is no convection heat transfer when the nanofilms are heated in such a vacuum. The circuit measuring the nanofilm electrical resistance is by a four-wire technique. The Ag glue is applied to connect the electrical wires with the leads. The measurement instruments include a power supply with constant current, a standard electrical resistance of  $100 \Omega$  and two multimeters. The temperature difference between the Au nanofilms and the liquid nitrogen cryostat is not more than 10 K. The heat loss of the nanofilms through radiation can therefore be ignored. Since the heat capacity of the Si substrate and the constant temperature shelf is very large and the heating power is only microwatts, the heat conduction in the suspended nanofilms is a one-dimensional case with uniform internal heat resource.

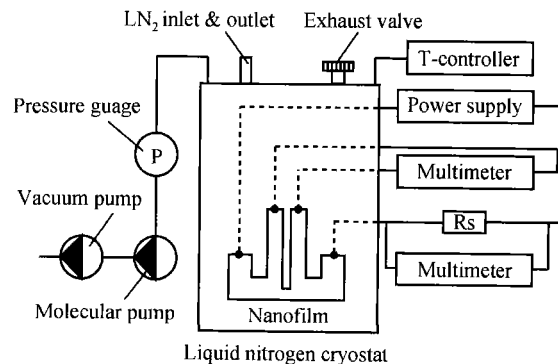


Fig. 2. Schematic diagram of the experimental setup measuring the thermal conductivity of the Au nanofilms.

## 1.2 Measurement mechanism

In measurements of the nanofilm thermal conductivity, the nanofilm serves both as a heating unit and as an electrical thermometer. Initially the nanofilm and the leads are maintained at thermal equilibrium at temperature  $T_0$ . With a heating power  $IU$ , where  $I$  and  $U$  are electrical current and voltage, respectively, the nanofilm appears to be subjected to one-dimensional heat transfer with uniform internal heat resource. The temperature distribution can analytically be expressed as

$$T = T_0 + \frac{IU}{2w d \lambda} x - \frac{IU}{2l w d \lambda} x^2, \quad (1)$$

where  $\lambda$  is the in-plane thermal conductivity of the Au nanofilm at  $T_0$ . Thus, the mean temperature of the nanofilm is

$$\bar{T} = T_0 + \frac{IU}{\lambda} \frac{l}{12wd}. \quad (2)$$

The nanofilm mean temperature is also associated with the electrical resistance and the temperature coefficient of resistance by

$$\bar{T} = T_s + \frac{R - R_s}{\beta R_s}, \quad (3)$$

where  $T_s = 273.2$  K is the datum temperature,  $R_s$  is the resistance of the Au nanofilm at 273.2 K,  $R$  is the nanofilm resistance, and  $\beta$  is the temperature coefficient of resistance of the nanofilm.

According to Eq. (2) and Eq. (3), we can obtain

$$R = R_0 + \frac{\beta R_s}{\lambda} \frac{l}{12wd} IU. \quad (4)$$

It indicates that the Au nanofilm resistance is proportional to the heating power under a given constant temperature condition. When the heating power goes to zero, the nanofilm resistance  $R_0$  at temperature  $T_0$  can be calculated by the intercept of the linear function  $R(IU)$ . Based on the calculated  $R_0$ , the temperature coefficient of resistance at  $T_0$  can then be obtained through Eq. (3). Defining the slope as  $k = \frac{\beta R_s}{\lambda} \frac{l}{12wd}$ , the in-plane thermal conductivity of the Au nanofilms can be calculated by

$$\lambda = \frac{R_0}{k} \frac{\beta}{1 + \beta(T_0 - T_s)} \frac{l}{12wd}. \quad (5)$$

## 2 Results and discussion

In order to steady the Au nanofilm microstructures and physical properties, a heat treatment at temperature 413.2 K for two hours was carried out before the measurement of the nanofilm thermal conductivity. The datum resistance at temperature 273.2 K was firstly measured to calculate the temperature coefficient of resistance. The datum resistances of samples a and b were respectively  $R_{sa} = 48.6 \Omega$  and  $R_{sb} = 59.8 \Omega$ . The measurement temperature in the present work ranged from 80 K to 300 K with an interval of 20 K.

Taking the nanofilm sample a as a case, the variation of the Au nanofilm resistance with the heating power is shown in Fig. 3 with the substrate being kept at constant temperatures of 100 K, 200 K and 300 K. The heating power in the measurements ranges from 1  $\mu$ W to 18  $\mu$ W. It is indicated that the Au nanofilm resistance is a linear function of the heating power, which agrees with Eq. (4) well. The

function can analytically be obtained by a least square method. The electrical resistances of the nanofilm sample a at 100 K, 200 K and 300 K are 31.17  $\Omega$ , 40.43  $\Omega$  and 50.88  $\Omega$ , respectively. It should be noted that the nanofilm electrical conductivity is much less than the corresponding bulk value due to the size effect.<sup>[10,11,13]</sup>

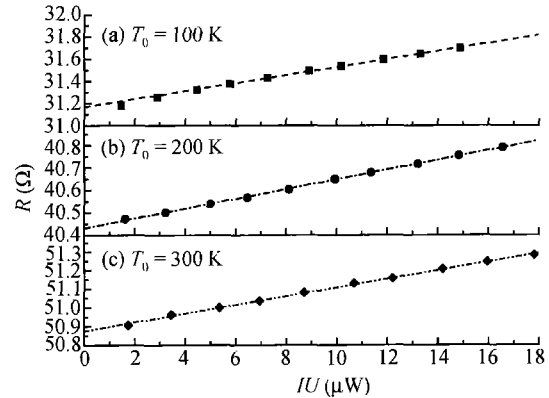


Fig. 3. Variations of the Au nanofilm resistance with the heating power at three different temperatures.

The temperature coefficient of resistance is defined as

$$\beta = \frac{R_0 - R_s}{R_s(T_0 - T_s)}. \quad (6)$$

The calculated temperature coefficient of resistance of the Au nanofilms at different temperatures is shown in Fig. 4. The experimentally measured temperature coefficients of resistance of the Au nanofilm a and b are appreciably different with a relative deviation of 20%. At 180 K, the temperature coefficient of resistance of the sample a is  $\beta_a = 1.80 \times 10^{-3} \text{ K}^{-1}$ , and the coefficient of the sample b is  $\beta_b = 1.45 \times 10^{-3} \text{ K}^{-1}$ . In the present experiment, the Au nanofilms are polycrystalline. The grain size relates to the fabri-

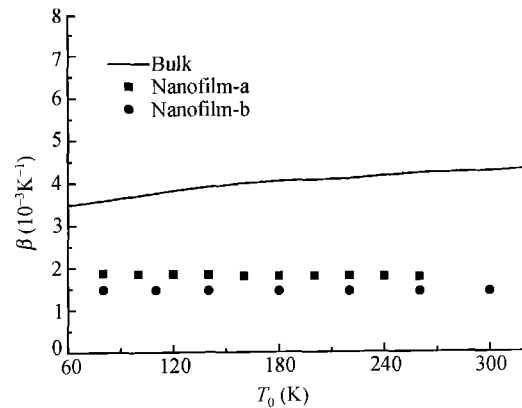


Fig. 4. Temperature coefficient of resistance of the Au nanofilms at different temperatures.

cation process greatly. The reason of the temperature coefficient difference between samples a and b may be that the grain sizes of the two samples are different. It is very important to note that the temperature coefficients of resistance of the two samples are both much less than that of the bulk Au. For example, the temperature coefficient of resistance of the bulk Au at 180 K is  $\beta_B = 4.03 \times 10^{-3} \text{ K}^{-1}$ , which is even two times larger than the measured coefficients of the 23 nm Au nanofilms.

Based on the obtained resistance and its temperature coefficient, the in-plane thermal conductivity of the Au nanofilms at different temperatures can be calculated by Eq. (5) (Fig. 5). For the 1DSSEH method, the uncertainty of the measured in-plane thermal conductivity is not more than 5%<sup>[10,13]</sup>. The measured in-plane thermal conductivity of the Au nanofilm a and b is appreciably different with a relative deviation of 25%. At 180 K, the in-plane thermal conductivity of the sample a is  $\lambda_a = 168.1 \text{ W} \cdot \text{m}^{-1} \cdot \text{K}^{-1}$ , and the thermal conductivity of the sample b is  $\lambda_b = 129.8 \text{ W} \cdot \text{m}^{-1} \cdot \text{K}^{-1}$ . The nanofilm in-plane thermal conductivity is affected not only by the surfaces but also by the grain boundaries. Though the thickness of the nanofilm a is the same as that of the sample b, they have different grain boundary effects due to different grain sizes. Thus, it is not difficult to understand the difference of the thermal conductivity between samples a and b. From Fig. 5, we can draw conclusions as follows: ① Strong size effects have been found on the measured nanofilm thermal conductivity. The in-plane thermal conductivity of the Au nanofilms is much less than that of the bulk material. For example, the bulk thermal conductivity of Au is  $\lambda_B = 329.9 \text{ W} \cdot \text{m}^{-1} \cdot \text{K}^{-1}$  at 180 K. In the present

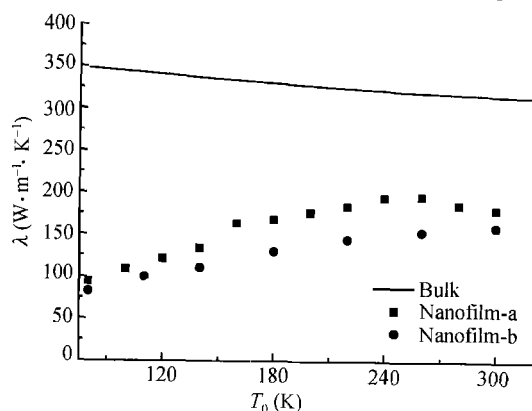


Fig. 5. In-plane thermal conductivity of the Au nanofilms at different temperatures.

work, however, the in-plane thermal conductivity of the Au nanofilms is less than half of the bulk value. ② The measured in-plane thermal conductivity of the Au nanofilms increases with the increasing temperature, which is opposite to the temperature dependence of the bulk property. ③ The difference of the thermal conductivities between the Au nanofilms and the bulk material increases with the decreasing temperature, which indicates that the size effect is more apparent at lower temperatures.

For the bulk metal material, the Wiedemann-Franz law shows that the thermal conductivity should be proportional to the electrical conductivity in the form of

$$L = \frac{\lambda}{\sigma T} \approx 2.44 \times 10^{-8} \text{ W} \cdot \Omega \cdot \text{K}^{-2}, \quad (7)$$

where  $L$  is the Lorenz number,  $\sigma$  is the electrical conductivity of a metal calculated by  $\sigma = l/(Rwd)$ . The Wiedemann-Franz law implies that the metal thermal conductivity can be calculated by the electrical conductivity. Some theoretical studies in literatures predicted that the thermal and electrical conductivities of thin films should agree with the Wiedemann-Franz law and the relationship of Eq. (7)<sup>[14–16]</sup>. In Refs. [10, 11], however, the ratio of the measured thermal and electrical conductivity of the Pt nanofilms with 15 nm and 28 nm in thickness was quite different from that of the bulk material. It was then concluded that the Wiedemann-Franz law cannot be applicable to Pt nanofilms. The Lorenz number of the Au nanofilms at different temperatures is shown in Fig. 6. It has been found that the Lorenz number of the Au nanofilms is much larger than the bulk value. For example, the Lorenz number of the bulk Au at 180 K is  $L_B = 2.34 \times 10^{-8} \text{ W} \cdot \Omega \cdot \text{K}^{-2}$ , while the Lorenz numbers of the Au nanofilm a and b are  $L_a = 6.86 \times 10^{-8} \text{ W} \cdot \Omega \cdot \text{K}^{-2}$  and  $L_b = 6.72 \times 10^{-8} \text{ W} \cdot \Omega \cdot \text{K}^{-2}$ , respectively. The Au nanofilm Lorenz number is about three times of the bulk value. In addition, the Lorenz number of the Au nanofilms in our experimental study was found to be temperature dependent. With the increasing temperature, the Lorenz number of the Au nanofilms decreases. In the present temperature range of 80–300 K, the Lorenz number variation of the nanofilm sample a was about  $1.03 \times 10^{-8} \text{ W} \cdot \Omega \cdot \text{K}^{-2}$ , and the variation of the sample b was about  $1.92 \times 10^{-8} \text{ W} \cdot \Omega \cdot \text{K}^{-2}$ , indicating that the thermal and electrical conductivities of metallic nanofilms do not follow the Wiedemann-Franz law due to the size effect.

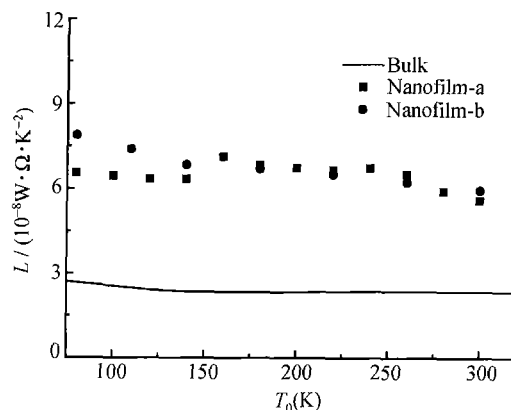


Fig. 6. Lorenz number of the Au nanofilms at different temperatures.

In fact, the Wiedemann-Franz law is a description of the contribution of electrons to the thermal and electrical conduction. However, the contribution of phonons to the thermal conduction is often excluded because it is relatively small. Since the Au nanofilms in the present study are polycrystalline, the grain boundary effect dominates the thermal and electrical properties of the nanofilms. When electron scattering takes place at the grain boundaries, the scattering electrons have almost no contribution to electrical conduction, while they can still enhance thermal conduction through transporting their energy to phonons. For polycrystalline metallic nanofilms, the phonon contribution increases compared with electrons, and the ratio of  $\lambda/\sigma T$  may deviate from the traditional Lorenz number. Therefore, the Wiedemann-Franz law is inapplicable for polycrystalline metallic nanofilms.

### 3 Conclusions

Two Au nanofilms with thickness of 23 nm were fabricated by the electron beam-physical vapor deposition method and a suspension technology. The nanofilm in-plane thermal conductivity was measured at 80–300 K by a one-dimensional steady-state electrical heating method. Strong size effects were found on the measured nanofilm thermal conductivity.

(1) The Au nanofilm in-plane thermal conductivity is much less than that of the bulk material. In the temperature range of 80–300 K, the in-plane thermal conductivity of the Au nanofilms is less than half of the bulk value.

(2) With the increasing temperature, the nano-

film thermal conductivity increases. This is opposite to the temperature dependence of the bulk property. It indicates that the size effect becomes stronger at lower temperatures.

(3) The Lorenz number of the Au nanofilms is about three times larger than the bulk value and decreases with the increasing temperature, which indicates the invalidity of the Wiedemann-Franz law for metallic nanofilms.

### References

- Tien C. L., Majumdar A. and Gerner F. M. *Microscale Energy Transport*. Washington D. C.: Taylor & Francis, 1997, 1–386.
- Chen G. *Heat transfer in micro- and nanoscale photonic devices*. *Annu. Rev. Heat Transfer*, 1996, 7: 1–57.
- Fujii M., Zhang X., Xie H. Q. et al. Measuring the thermal conductivity of a single carbon nanotube. *Phys. Rev. Lett.*, 2005, 95: 065502.
- Zhang X., Fujiwara S. and Fujii M. Measurements of thermal conductivity and electrical conductivity of a single carbon fiber. *Int. J. Thermophys.*, 2000, 21(4): 965–980.
- Vashaee D. and Shakouri A. Improved thermoelectric power factor in metal-based superlattices. *Phys. Rev. Lett.*, 2004, 92(10): 106103.
- Fukushima A., Yagami K., Ashwin A. et al. Peltier effect in sub-micron-size metallic junctions. *Jap. J. Appl. Phys.*, 2005, 44(1): L12–L14.
- Cahill D. G., Ford W. K., Goodson K. E. et al. Nanoscale thermal transport. *J. Appl. Phys.*, 2003, 93(2): 793–818.
- Feng X. L., Li Z. X., Liang X. G. et al. Molecular dynamics study on thermal conductivity of nanoscale thin films. *Chin. Sci. Bull.*, 2001, 46(7): 604–607.
- Heino P. and Ristolainen E. Thermal conduction at the nanoscale in some metals by MD. *Microelectro. J.*, 2003, 34: 773–777.
- Zhang X., Xie H. Q., Fujii M. et al. Thermal and electrical conductivity of a suspended platinum nanofilm. *Appl. Phys. Lett.*, 2005, 86(17): 171912.
- Zhang X., Zhang Q. G., Cao B. Y. et al. Experimental studies on thermal and electrical properties of platinum nanofilms. *Chin. Phys. Lett.*, 2006, 23(4): 936–938.
- Ashcroft N. W. and Mermin N. D. *Solid State Physics*. New York: Holt, Rinehart and Winston, 1976, 1–826.
- Zhang X., Fujii M., Takahashi K. et al. Measurements of in-plane thermal conductivity and electrical conductivity of suspended platinum thin film. In: *Proceedings of the 26th Japan Symposium on Thermophysical Properties*, Tokyo, Japan, 2005, 349–356.
- Tellier C. R. and Tosser A. J. *Size Effects of Thin Films*. New York: Elsevier, 1982, 1–310.
- Clemens B. M., Eesley G. L. and Paddock C. A. Time-resolved thermal transport in compositionally modulated metal films. *Phys. Rev. B*, 1988, 37: 1085–1096.
- Stewart D. and Norris P. M. Size effects on the thermal conductivity of thin metallic wires: microscale implications. *Microscale Thermophys. Eng.*, 2000, 4: 89–101.